

Investigation of the growth process of organic/inorganic doped aromatic derivatives crystals

A. STANCULESCU

National Institute for Materials Physics, 105bis Atomistilor Street, P.O.Box MG 7,
077125 Magurele, Bucharest, Romania

This paper presents a study of the thermal regime associated with the experimental configuration used for the growth of doped organic crystals from the melt in Bridgman-Stockbarger configurations. For different systems, host: meta-dinitrobenzene (m-DNB), benzil/guest: m-DNB, naphthalene, iodine, I have investigated the effect of the changes in the experimental conditions (dopant type and concentration, $c=0.5-3$ wt %, thermal gradient at the growth interface, $\Delta T=6-33^\circ\text{C}$, moving speed of the solid-liquid interface, $V=0.7-2.7$ mm/h) on the crystals growth process. I have made comparisons between the particularities of the incorporation mechanism of the big acceptor (atom:iodine $c=0.5$; 1; 2 wt %; molecule: m-DNB and naphthalene $c=1.5$; 3 wt %) and dopant segregation mechanism, and the transmission properties of different monocomponent crystalline organic matrix (m-DNB and benzil). I have also investigated the influence of the simultaneous presence of two dopants (m-DNB or naphthalene/iodine) in organic benzil matrix and their effect on the optical properties. I have evaluated the growth interface stability in our Bridgman-Stockbarger experimental configuration and analysed the conditions for the generation of the morphological instabilities in benzil-dopant system.

(Received November 14, 2006; accepted April 12, 2007)

Keywords: Organic compounds, Meta-dinitrobenzene, Benzil, Crystals growth, Dopants, UV-VIS Spectroscopy, Morphological instability

1. Introduction

In the last decades, organic materials have been considered as potential substitutes for inorganic semiconductor in optical [1-3] and opto-electronical [4-6] applications. The interest for studying organic crystals can also be justified by the perspective to use these materials as crystalline host matrices for organic or inorganic guests.

The investigation of the effect of the dopant incorporation and organization within the organic matrix on the lattice properties could be a step in obtaining a new class of materials that may combine the advantageous properties of both organic and inorganic component. The presence of the inorganic component can improve some properties as electrical mobility, thermal stability and magnetic and dielectric transitions. The organic matrices can assure an efficient fluorescence mechanism, a simple processing and also can contribute to the electrical transport properties. The homogeneous doping of organic crystalline materials is difficult because of their low melting point, supercooling phenomenon, low thermal conductivity [7,8], but is favoured by the weak bonding forces between molecules [9].

There are not too many references on the doped aromatic derivatives crystals growth exception on the crystals doped with rare earth metallic ions as materials for luminescent and laser applications [10,11]. The effect of other metallic dopants on the properties of the organic

crystals has not been intensively studied till now except the effect of cadmium ions [10] and sodium and silver ions on the properties of benzil crystals [12-14]. The information is even poorer in the field of organic doping of organic matrix [12,15,16].

This paper presents some experimental and theoretical contributions concerning the growth process of organic/inorganic doped substituted aromatic derivatives molecular crystals: m-DNB and benzil.

2. Experimental methods

Because m-DNB, benzil and naphthalene are characterized by a good thermal stability at the melting point we have used for crystal growth the Bridgman-Stockbarger method in a simplified experimental configuration (Figure 1,a) that assures steep gradients at the melt-crystal interface (Figure 1,b) using a double quartz walls heater with variable spacing between the coils to control the thermal gradient, and a third quartz tube for better insulation from the outside environment. The temperature is adjusted by a temperature control system connected with a thermocouple that indicates the hot zone temperature. Experimental conditions used to grow organic pure and doped crystals are listed in Table 1. The starting material, previously purified, is introduced in a glass ampoule that is sealed under vacuum. A special clock mechanism is used to slowly move the ampoule in the furnace.

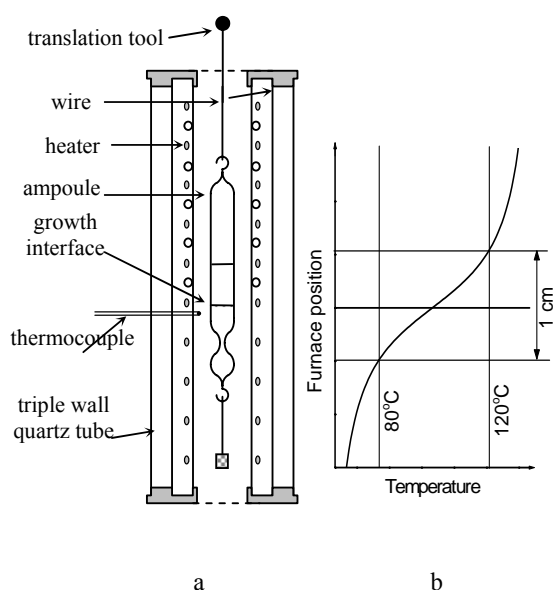


Fig. 1. Experimental set-up for organic crystals growth (a).
Thermal profile of the furnace (b).

Table 1. Experimental conditions for growing *m*-DNB and benzil pure and doped crystals.

| Organic compound:dopant | Hot zone temperature (°C) | Thermal gradient at the growth interface $ \Delta T $ (°C/cm) | Moving speed of the interface V(mm/h) |
|---|---------------------------|---|---------------------------------------|
| Benzil pure [17] | 112 | 24-28 | 1,7-2,1 |
| Benzil: iodine (1 wt %) | 116 | 25-30 | 1.6-2 |
| Benzil: iodine (2 wt %) | 113 | 25-30 | 1.9-2.3 |
| Benzil: <i>m</i> -DNB(3 wt %) | 108 | 24-28 | 1,6-2 |
| Benzil: <i>m</i> -DNB (1 wt %)+ iodine (0.5 wt %) | 115 | 25-30 | 1.5-1.9 |
| Benzil: <i>m</i> -DNB (1 wt %)+ iodine (1 wt %) | 115 | 23-27 | 2.1-2.5 |
| Benzil:naphthalene (1.5 wt %) | 114 | 24-28 | 2.3-2.7 |
| Benzil:naphthalene (1 wt %)+iodine (1 wt %) | 114 | 25-30 | 1.8-2.2 |
| <i>m</i> -DNB pure [18] | 115 | 6-11 | 0,7-1 |
| <i>m</i> -DNB: iodine (1 wt %) | 117 | 29-33 | 2.3-2.7 |
| <i>m</i> -DNB:iodine (2 wt %) | 112 | 25-30 | 1.8-2.2 |

3. Results and discussion

Benzil and *m*-DNB crystals present tendency to supercooling and low thermal conductivity and are characterized by high enthalpy of fusion ($\Delta_f H = 23.56$ kJ/mol for benzil [19] respectively 17.36 kJ/mol for *m*-DNB [20]). The high values 4.6×10^{24} mol⁻¹ respectively 3.5×10^{24} mol⁻¹ computed for the ratio ($\Delta_f H / k \cdot T_m$), where k is the Boltzmann constant and T_m is the melting temperature of the compounds, sustain a tendency to faceted growth morphology and high constitutional supercooling [21] that must be compensated by a steep gradient at the crystal/melt interface. The

We have chosen a conical shape of the crucible/ampoule tip with a narrower zone (Figure 1,a) that offers the possibility to avoid the suddenly freezing of the melt situated in the narrower zone that could lead to the propagation of the polycrystalline solid through the whole volume of the melt, and consequently to control the nucleation and solidification processes. The disadvantage of this configuration is the selection of a low growth rate direction that favours the subsequent nucleation above the narrower zone of the tip.

Bulk sample UV-VIS transmission spectra and FTIR spectra of the thin film samples prepared from pure and doped organic materials melted between two silicon wafers have been realized with a computer assisted double beam Perkin-Elmer Lambda 25 Spectrophotometer respectively Perkin-Elmer BX1 Spectrophotometer.

thermal transfer near the interface is controlled by thermal conduction, the convection being reduced through the use of small diameters (<15 mm) ampoules.

The compositional homogeneity and crystalline structure are determinate by the macroscopic shape of the interface between the solid and liquid phase during the directional solidification, which is the result of the conjugated action of different factors as the thermal regime, the moving speed of the growth ampoule and the anisotropic growth speed. Because pure melted benzil and *m*-DNB are transparent light yellow respectively white-yellow materials has been used a transparent furnace for a direct visualization, in real time, of the interface shape as a parameter of the growth process and an indicator for subsequent control of the crystal quality.

By repeated crystallization experiments we have identified the thermal growth conditions as a compromise between the gradient necessary to compensate the supercooling and that necessary to avoid the faceting process [21]. In the configuration mentioned above, most of the latent melting heat is removed through the growing crystal characterized by low thermal conductivity (e.g. $2.63 \times 10^{-3} \text{ W} \cdot \text{cm}^{-1} \cdot ^\circ\text{C}$ for benzil crystals [22]), that involves longer time for solidification and as consequence low macroscopic moving speed of the ampoule in the heater (rough estimation of the moving speed of the growth interface) of 0.7-2.7 mm/h (Table 1).

The growth process is close to the stationary growth assuring a uniform distribution of the temperature field and a steeper temperature gradient at the growth interface. A reduced curvature of the melt-solid interface is obtained by a correct emplacement of the ampoule in the thermal field to avoid a concave surface of the growing crystal, favourable to the grains boundaries generation. Increasing the thermal gradient at the liquid-solid interface in the Bridgman-Stockbarger configuration for pure melts, to $\Delta T = 28^\circ\text{C}$ for benzil and to $\Delta T = 11^\circ\text{C}$ for m-DNB, the growth interface moves in the cold zone and has a convex shape of the crystal surface, favourable to the germ selection and growth of crystals with better optical properties [18].

The mechanisms of incorporation or rejection of the impurity particles at the interface during the solidification process are correlated with the thermal field and the interface moving speed to assure the engulfment of the foreign particles by the crystallisation front. The rejected particles create a layer enriched in foreign particles in front of the interface and generate compositional variations and micrononhomogeneities as growth striations. For iodine doped m-DNB and benzil crystals it has been obtained an inclined shape of the solidification interface because the melt situated at higher temperature (the ampoule wall is situated near the heater wall) solidify later than the melt situate at lower temperature (the ampoule wall is far from the heater wall). The nonuniform thermal field and the radial gradient of the temperature in the growth ampoule that is deviated from the axial position in the heater could partially explain this shape of the liquid-solid interface. The shape of the interface has generated a polycrystalline structure of the ingot with large grains zones alternating with small grains zones. At high concentration of impurity (2 wt % iodine in benzil or iodine in m-DNB) it is necessary a lower moving speed of the interface (Table 1) to control the incorporation of the impurity in the matrix lattice. To grow benzil crystals simultaneously containing two dopants, m-DNB/naphthalene and iodine (Table 1), it was selected a thermal gradient between $23\text{-}30^\circ\text{C}$ at the solid-liquid interface (Table 1) in correlation with the components of the dopant/matrix system to avoid the instant propagation of the solification

front above the neck of the ampoule and the development of a glassy structure. A slow moving speed between 1.5-2.2 mm/h of the growth interface (Table 1) has been used to favour the evacuation of the latent melting heat.

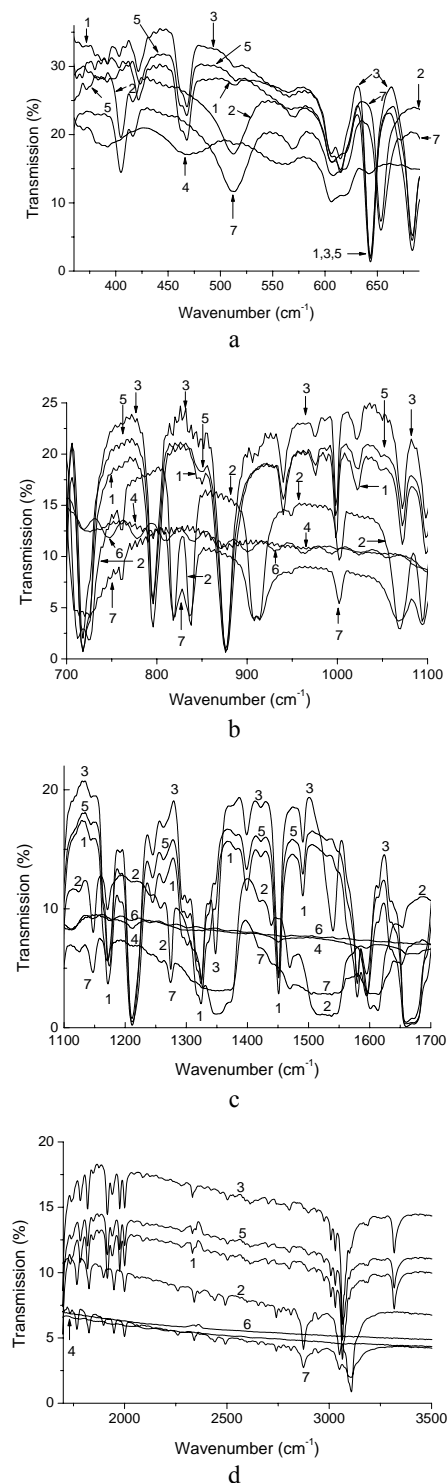


Fig. 2 IR Spectra (on different spectral ranges) of pure and doped benzil and m-DNB films grown between two

silicon wafers: 1: benzil; 2: *m*-DNB; 3: benzil+*m*-DNB; 4: benzil + naphthalene; 5: benzil + I₂ (1 wt %); 6: reference sample (Si wafers); 7: *m*-DNB+I₂ (2 wt %).

The factors affecting the dopant incorporation in the host lattice are the shape, volume and intermolecular bonds of the dopant molecules. Benzil belongs to the trigonal trapezohedral class and has three molecules helically disposed and closed packed around the 3₁ axe [23]. In *m*-DNB the smallest distance between the O atoms and the CH groups of the adjacent molecules varies between 2.9 Å and 3.3 Å [24,25]. All the other distances between two neighbour O atoms or CH groups are greater and vary between 3.2 Å and 3.7 Å, respectively 3.6 Å and 3.8 Å [24,25]. From the molecular structure and geometrical considerations I have evaluated the approximate diameter of the free space in benzil [13] and *m*-DNB around 2.9 Å. From geometrical considerations iodine atom/ion can penetrate the benzil and *m*-DNB lattices and most probably can be localised in interstitial void sites, the incorporation being somehow facilitated by the local deformation in the organic solids characterised by weak van der Waals bonds.

Because in the IR spectra of iodine doped *m*-DNB samples (Fig. 2 curve 7) and *m*-DNB/naphthalene/iodine doped benzil samples (Fig. 2 curves 3,4,5) changes related to new absorption peaks situated at wavenumbers that correspond to new bonds have not been emphasised, we presume that no chemical reactions took place between the components of the dopant/matrix systems. The most important effect was the broadening of the absorption peaks (no their shift), more pronounced in naphthalene doped benzil crystals (Fig. 2 curve 4). Iodine has a strong acceptor character as the carbonyl groups in benzil and nitro groups in *m*-DNB and as a consequence it is not possible a charge transfer between the substituent groups in *m*-DNB or benzil on one hand and metallic iodine on the other. So the possibilities of chemical reaction or charge transfer between benzil/*m*-DNB (matrix) and iodine (dopant) have been excluded.

Even in the absence of the chemical reactions, the high first ionisation enthalpy for iodine atoms ($\Delta_1H=1008.4$ kJ/mol) is favourable to cluster generation and no to incorporation of isolated atoms [26]. This tendency for clustering can create difficulties in iodine incorporation in benzil and *m*-DNB, perturbing the lattices and generating defects as cracks.

The behaviour of the organic dopants is different in different matrices. Because the organic molecules are big they cannot be included interstitially in the host lattice but only substitutionally respecting the condition for solubility in the solid phase and the geometrical similarity criterion [27,28] that involves the geometrical dimension matching between the dopant and matrix molecules. If there are geometrical differences between the host/guest organic molecules, the substitutional replacement of the host molecule with a guest one is less probable and the distortion of the host crystalline lattice can generate dopant microinclusions and cracks.

A measure of the geometrical similarity is the overlapping factor expressed as the ratio between the overlapped and overlapped volume of the two

components, host molecule/dopant molecule, and offers the possibility to estimate the doping level allowed for each host/guest system [29] (low value of this ratio correspond to low doping level of the organic matrix).

Supposing a spherical shape for the organic molecule and taking into account the length of the chemical bounds involved in the investigated compounds, I have estimated the volume of *m*-DNB, benzil and naphthalene molecule. Because the volume of the matrix benzil molecule is much greater than that of the dopant (*m*-DNB molecule) the nonoccupied computed volume is much greater than the occupied volume ($V^{no}/V^o \sim 8.5 \gg 1$) and the probability for *m*-DNB to occupy substitutional position replacing the benzil molecules is very small. As a consequence *m*-DNB molecules, which are not completely dissolved in the host matrix segregate as a distinct phase in benzil matrix generating microinclusions that favours the light scattering in benzil crystals nonhomogeneously doped with *m*-DNB. A weaker segregation effect is observed in benzil crystals doped with naphthalene because the geometrical differences are smaller in this case ($V^{no}/V^o \sim 2 > 1$).

These assumptions concerning the dopant segregation effect are confirmed by UV-VIS transmission measurements. The transmission of benzil doped with *m*-DNB (P3) is lower than the transmission of benzil doped with naphthalene (P2), for the same thickness (#2 mm) of the samples suggesting a stronger segregation process for *m*-DNB than for naphthalene in the benzil matrix (Fig. 3a).

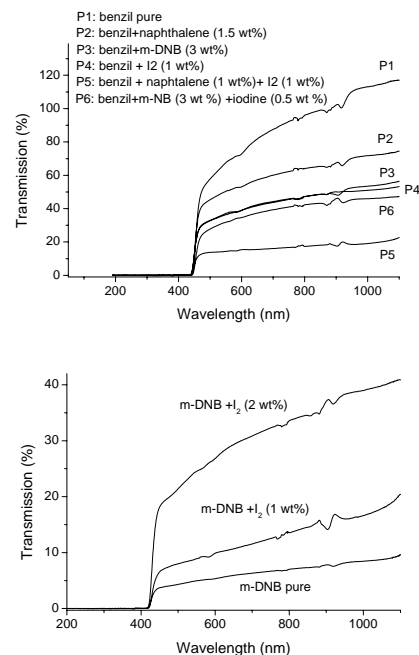


Fig. 3. The effect of the dopants segregation on the UV-VIS transmission spectra of the benzil and *m*-DNB matrix.

Supposing the same degree of surface processing, the transmission is lower in benzil simultaneously doped with naphthalene and iodine (#1.4 mm) compared to benzil simultaneously doped with *m*-DNB and iodine, (#3.2 mm)

(Figure 3a). This suggests stronger iodine segregation with effect on the sample homogeneity in the presence of naphthalene (P5) than of m-DNB (P6). The segregation of iodine (Fig. 3a) is less significant in the absence of any other organic impurity in the benzil matrix (P4).

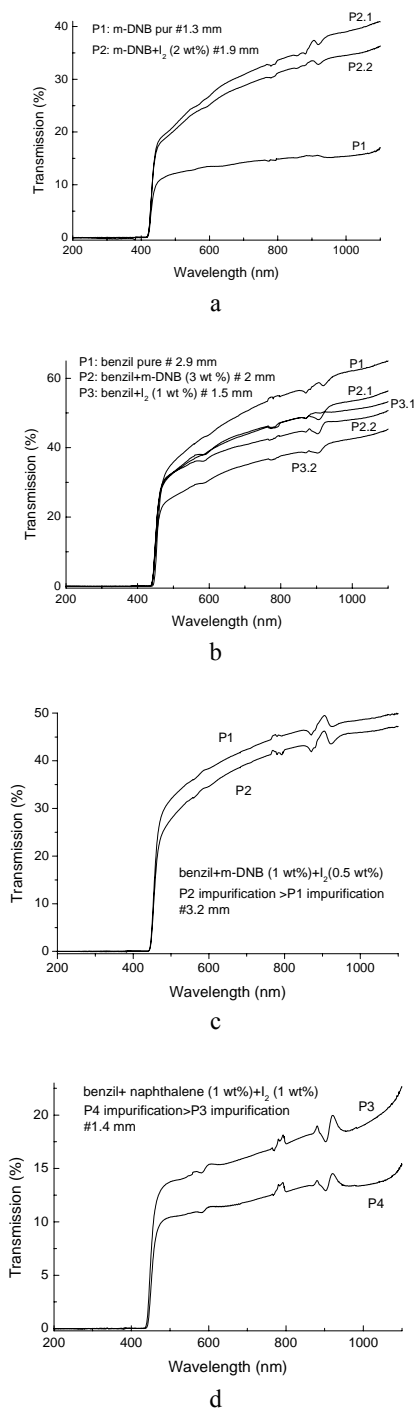


Fig. 4. Transmission variations associated with compositional nonhomogeneities in doped organic crystals: radial transmission variations across the wafer: a, b; longitudinal transmission variation along the ingot: c, d. The impurification increases in the following

succession: $P2 > P1$ and $P4 > P3$.

The position and the shape of the fundamental absorption edge was not significantly changed by m-DNB, naphthalene or iodine in benzil (Figure 5a) and by iodine in m-DNB (Figure 5b), confirming the same behaviour previously mentioned for benzil crystals doped with sodium and silver [13].

Radial and longitudinal variations in the homogeneity of the samples (Fig. 4) have been emphasised by UV-VIS transmission measurements in different points on the same wafer respectively on wafers with different localisation along the ingot. The experimental thermal regime was adequate for the generation of nonhomogeneous binary solid solution of m-DNB doped with 2 wt % iodine (Figure 4a), benzil doped with 3 wt % m-DNB and benzil doped with 1 wt % iodine (Figure 4b) reflected in radial nonhomogeneities of the samples. The decrease of the transmission associated with the increase in the impurification degree and longitudinal nonhomogeneities is observed for the last freezing end enriched in foreign particles of the benzil simultaneously doped with m-DNB and iodine (Fig. 4c) or naphthalene and iodine (Fig. 4d).

The study of the stability aspects of the solid-liquid interface in doped benzil and m-DNB binary solidification process is important because deteriorations in the crystal homogeneity can appear as a result of the morphological instability of the growth interface in the settled experimental conditions.

The investigated organic systems are characterised by a low thermal conductivity in the solid phase and high value of the solidification enthalpy, which has to be continuously liberated during the crystallization process. Many flow cells can be developed in the matrix/dopant (solvent/solute) melt leading to a nonuniform distribution of the dopant in the matrix. Doped organic melt are characterized by constitutional supercooling because the impurity rejected by the freezing solid can accumulate ahead of the advancing solid-liquid interface so that the equilibrium freezing temperature of the liquid adjacent to the interface is above the actual temperature and the gradient of the equilibrium temperature is given by

$$\Delta T_e = \Delta C \cdot m \quad (1)$$

where ΔC =concentration gradient at the interface and m =slope of the liquidus line. By convention, the product $\Delta C \cdot m > 0$ and for an impurity rejected from the interface that depress the melting temperature, $m < 0$ [30]. This phenomenon can generate an unstable solid-liquid interface because a protuberance situated at the interface has the tendency to grow spontaneously and can be compensated by low moving speed of the interface or steep temperature gradients, conditions satisfied by the experimental configuration. From stability considerations, m-DNB and naphthalene segregation in benzil takes place under conditions that favour the breakdown of the solid/liquid interface.

I have discussed the simpler case of one impurity soluble in the solid phase [9] (m-DNB in benzil, naphthalene in benzil, iodine in benzil and iodine in

m-DNB) that shifts the freezing temperature of the matrix (benzil or m-DNB). Naphthalene ($T_m=80^\circ\text{C}$) and m-DNB ($T_m=90^\circ\text{C}$) impurities are not readily incorporated into the crystal lattice and therefore depress the melting point of the pure benzil ($T_m=95^\circ\text{C}$) and the slope of the liquidus line is $m<0$. The segregation coefficients of naphthalene in benzil and m-DNB in benzil are $k<1$. Because $m<0$, naphthalene and m-DNB are rejected from the growth interface and incorporated with difficulty in the growing crystal of benzil. They accumulate in front of the crystal generating an instability of the growth surface.

Iodine rises the melting point of benzil and m-DNB and is easier incorporated in their lattices because these systems have a wide range of homogeneous miscibility [9] in the solid state (with high dopant acceptability and the segregation coefficient $k>1$).

In benzil matrix simultaneously doped with two dopants in low concentration (diluted systems), the interaction among the impurities is negligible compared to the interaction of individual impurity molecule with the host, but sometimes a mutual influence can exist for k not very different from 1 so that a second impurity switches the segregation coefficient from $k<1$ to $k>1$ [9].

The interface stability problem was studied using the Mullin-Sekerka [30-35] criterion that fixes the stability limits of the growth interface and the conditions necessary to initiate instabilities:

$$Sk \equiv \frac{(V \cdot \rho_m \cdot \Delta_f H - (k_m - k_s) \cdot \Delta T)}{(k_m + k_s) \cdot (\Delta T + \Delta C \cdot m)} \geq 1 \quad (2)$$

where V =ampoule moving speed, ρ_m =melt benzil density, k_m =thermal conductivity for the melt benzil, k_s =thermal conductivity for benzil crystal, $\Delta_f H$ =enthalpy of solidification, ΔT =thermal gradient, ΔC = concentration gradient at the growth interface and m =slope of the liquidus curve. For our system in mentioned experimental conditions (Table 1) this stability condition became:

$$\Delta C \cdot m \leq 10.0727 \cdot V - 0.4382 \cdot \Delta T \quad (3),$$

where $\Delta T<0$ because $T_{\text{final}}<T_{\text{initial}}$ (solidification process).

In the system benzil/dopant and settled experimental conditions defined by the thermal gradient at the interface ($|\Delta T|$) and moving speed of the interface (V), the zones corresponding to stable and unstable growth have been delimited drawing the curves $\Delta C \cdot m = f(|\Delta T|)$ for $V=\text{constant}$ (Fig. 5). For given ΔT and V , the dependence between the concentration gradient at the growth interface and the slope of the liquidus line has been evaluated for a stable growth process. For all the investigated growth systems, for chosen temperature gradient and moving speed (Table 1), the system is situated in the stable growth zone, below the curve given by eq. (3) (Figure 5). We have emphasised that for high concentration gradients (ΔC), the system moves in the unstable growth zone, above the curve given by eq. (3),

generating an increase in the morphological instability and as consequence less homogeneous crystal (Figure 5). The curves $\Delta C \cdot m = f(V)$ for $\Delta T=\text{const.}$ have been drawn and have been established the stable and unstable growth zone satisfying the condition $\Delta C \cdot m \geq 0$ for our experimental configurations and systems (Fig. 6).

For a given thermal gradient at the interface, a variation of the interface moving speed between 0.07 - 0.27 cm/h has no significant influence on the area of the stable growth delimited by the growth parameters (Figure 5). The area of the stable growth zone increases significantly with the increase of the thermal gradient for a given moving speed of the interface and the system remains in the stable growth zone even for increased concentration gradient at the interface (Figure 6). These considerations are useful in choosing the most adequate parameters for a stable growth process to obtain homogeneous crystals.

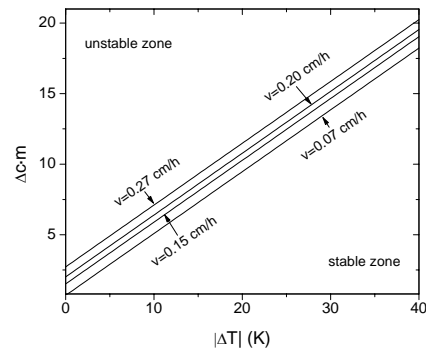


Fig. 5. Stable (above the curves) and unstable (below the curves) growth zones for benzil/dopant system in Bridgman - Stockbarger configuration delimited by the following curves: $\Delta C \cdot m = f(|\Delta T|)$, $V=\text{const.}$

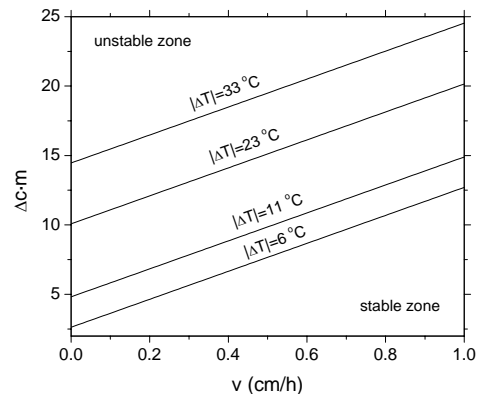


Fig. 6. Stable (above the curves) and unstable (below the curves) growth zones for benzil/dopant system in Bridgman - Stockbarger configuration delimited by the following curves $\Delta C \cdot m = f(V)$, $|\Delta T|=\text{const.}$

For our benzil crystals, because $k_m > k_s$ [32], the term $(k_m - k_s) \cdot \Delta T / (k_m + k_s)$ in eq.(2) assures a wider range of values (situated in the stable growth zone) for the product $\Delta C \cdot m$ that makes the interface more stable.

The growth regimes for the investigated systems are comparable from the point of view of interface stability because there are not significant differences in the values of the ratio $|\Delta T|/V$ [30].

Table 2. $|\Delta T|/V$ ratio for our systems and experimental configurations.

| Experimental matrix/dopant system | Experimental conditions | $\frac{ \Delta T }{V} \times 10^6$ ($^{\circ}\text{C cm}^{-2}\text{s}$) |
|---|-------------------------------------|---|
| Benzil pure | 25.9 $^{\circ}\text{C}$; 0.19 cm/h | 0.50 |
| Benzil: iodine (1 wt %) | 27.5 $^{\circ}\text{C}$; 0.18 cm/h | 0.50 |
| Benzil: iodine (2 wt %) | 27.5 $^{\circ}\text{C}$; 0.21 cm/h | 0.47 |
| Benzil:m-DNB (3 wt %) | 25.9 $^{\circ}\text{C}$; 0.18 cm/h | 0.51 |
| Benzil:m-DNB (1 wt %)+ iodine (0.5 wt %) | 27.5 $^{\circ}\text{C}$; 0.17 cm/h | 0.58 |
| Benzil:m-DNB (1 wt %)+ iodine (1 wt %) | 25.0 $^{\circ}\text{C}$; 0.23 cm/h | 0.39 |
| Benzil+naphthalene (1.5 wt %) | 26.0 $^{\circ}\text{C}$; 0.25 cm/h | 0.37 |
| Benzil:naphthalene (1 wt %)+iodine (1 wt %) | 27.5 $^{\circ}\text{C}$; 0.20 cm/h | 0.49 |
| m-DNB pure | 8.5 $^{\circ}\text{C}$; 0.07 cm/h | 0.43 |
| m-DNB:iodine (1 wt %) | 31.0 $^{\circ}\text{C}$; 0.25 cm/h | 0.44 |
| m-DNB: iodine (2 wt %) | 27.5 $^{\circ}\text{C}$; 0.20 cm/h | 0.49 |

From the morphological stability considerations, the inclined melt-crystal interface emphasised in m-DNB and benzil doped with iodine systems can be explained taking into account the thermal gradient and the effect of the component of the interfacial solid-liquid tension in an ampoule whose symmetry axis forms a sharp angle with the furnace axis.

4. Conclusions

For different organic host (m-DNB, benzil)/guest (organic: m-DNB, naphthalene or/and inorganic, iodine) systems have been defined the experimental conditions (dopant concentration $c=0.5-3$ wt %, thermal gradient at the growth interface $\Delta T=6-33$ $^{\circ}\text{C}$, moving speed of the solid-liquid interface $V=0.7-2.7$ mm/h) to obtain crystals from the melt in Bridgman-Stockbarger configurations.

Some differences between the effects of inorganic (incorporated interstitially) and organic (incorporated substitutionally) dopants on the optical properties of the benzil and m-DNB crystalline matrix have been remarked, emphasising the nonhomogeneities generation associated with the segregation process in matrix/dopant systems. We concluded a stronger effect of the nonhomogeneities induced by m-DNB than by naphthalene inclusions in benzil, and a stronger iodine segregation in the presence of naphthalene than of m-DNB.

No significantly changes in the position and the shape of the fundamental absorption edge was evidenced in iodine

doped m-DNB and m-DNB, naphthalene or iodine doped benzil excluding any chemical reaction or charge transfer between matrix and dopant.

Applying the Sekerka criterion has deduced that all the investigated growth systems are situated in the stable growth zone for the given temperature gradient and moving speed, showing no accentuated instability of the growth interface. The morphological instability became significant for high concentration gradients at the solid-liquid interface.

The inclined shape of the solidification interface obtained for iodine doped benzil and m-DNB crystals was associated with a nonuniform thermal field and the effect of the interfacial solid-liquid tension.

All the growth regimes investigated are similar from the point of view of the liquid-solid interface stability criteria because the ratio between the thermal gradient and the moving speed of the interface are comparable ($0.3-0.6 \times 10^6$ $^{\circ}\text{C cm}^{-2}\text{s}$).

References

- [1] J. Zyss, D. S. Chemla, in "Nonlinear Optical Properties of Organic Molecules and Crystals", D. S. Chemla, J. Zyss Eds., Academic Press Inc., Orlando (1987).
- [2] Ch. Bosshard, K. Sutter, Ph. Prêtre, J. Hüller, M. Flörsheimer, P. Kaatz, P. Günter, "Organic Nonlinear Optical Materials in "Advances in Nonlinear Optics", vol.1, Gordon Breach Publishers, Switzerland (1995).
- [3] P. N. Prasad, D. J. Williams, "Introduction to nonlinear optical effects in molecules and polymers", John Wiley & Sons Inc. (1991).
- [4] C. W. Tang, S. A. Van Slyke, Appl. Phys. Lett. **51**, 913 (1988).
- [5] J. R. Sheats, H. Antoniadis, M. Hueschen, W. Leonard, J. Miller, R. Moon, D. Roitman, A. Stocking, Science **273**, 884 (1996).
- [6] W. Riess, H. Riel, T. Beierlein, W. Brütting, P. Müller, P. F. Seidler, IBM J. Res. & Dev. **45**, 77 (2001).
- [7] G. F. Reynolds, in: D. Fox, M. M. Labes, A. Weissberger (Eds.), Physics and Chemistry of the Organic Solid State, vol.1, Interscience, New York, 1963, p.267.
- [8] A. Périgaud, Bull. Soc. Sci. Bretagne **48** (Hors Série) 57 (1973).
- [9] N. Karl, High purity organic molecular crystals, in: H.C. Freyhardt (Ed.), Crystals: Growth, Properties and Applications, vol. 4, Springer, Berlin, 1980, p.1.
- [10] W. S. Wang, M. D. Aggarwal, J. Crystal Growth **128**, 891 (1993).
- [11] M. A. Noginov, M. Curley, N. Noginova, W. S. Wang, M. D. Aggarwal, Appl. Opt. **37**, 5737 (1998).
- [12] A. Stanculescu, S. Antohe, H. V. Alexandru, L. Tugulea, F. Stanculescu, M. Socol, Synthetic Metals, **147**, 215 (2004).

- [13] A. Stanculescu, I. Tugulea, H. V. Alexandru, F. Stanculescu, M. Socol, *J. Crystal Growth* **275**, e1779 (2005).
- [14] F. Stanculescu, A. Stanculescu, M. Socol, *J. Optoelectron. Adv. Mater.* **8**, 1053 (2006).
- [15] A. Stanculescu, F. Stanculescu, H. Alexandru, *Journal Crystal Growth*, **198/199**, 572 (1999).
- [16] A. Stanculescu, F. Stanculescu, M. Socol, *J. Optoelectron. Adv. Mater.* **8**, 1057 (2006).
- [17] A. Stanculescu, L. Tugulea, F. Stanculescu, M. Socol, *Analele Universitatii Bucuresti, Fizica*, **LIII**, 15 (2004).
- [18] A. Stanculescu, F. Stanculescu, *J. Optoelectron. Adv. Mater.* **2**, 536 (2000).
- [19] E. S. Domalski, E. D. Hearing, *J. Phys. Chem. Ref. Data*, **1** (1996).
- [20] W. E. Acree Jr., *Thermochim. Acta*, **37** (1991).
- [21] N. B. Singh, T. Henningsen, *J. Cryst. Growth* **128**, 976 (1993).
- [22] C. W. Lang, C. R. Song, *J. Crystal Growth* **180**, 127 (1997).
- [23] C. J. Brown, R. Sadanaga, *Acta Cryst.* **18**, 158 (1965).
- [24] E. M. Archer, *Proc. Roy. Soc.* **A188**, 51 (1946).
- [25] J. Trotter, *Acta Cryst.* **14**, 244 (1961).
- [26] Y. Hirose, A. Kahn, *Appl. Phys. Lett.* **68**, 217 (1996).
- [27] A. I. Kitaigorodski, *Molecular Crystals and Molecules* (Academic Press, New York, 1973).
- [28] A. I. Kitaigorodski, *J. Chem. Phys.* **63**, 9 (1966).
- [29] P. J. Halfpenny, R. I. Ristic, E. E. A. Shepherd, J. N. Sherwood, *J. Crystal Growth* **128**, 970 (1993).
- [30] R. F. Sekerka, *J. Cryst. Growth*, **3**(4), 71 (1968).
- [31] W. W. Mullins, R. F. Sekerka, *J. Appl. Phys.* **34**, 323 (1963).
- [32] W. W. Mullins, R. F. Sekerka, *J. Appl. Phys.* **35**, 444 (1964).
- [33] R. L. Paker, *Crystal Growth Mechanism: Energetics, kinetics and Transport in Solid State Phys.* Science Press Inc. Tokyo (1970), vol. 25, p. 151.
- [34] M. C. Flemings, "Solidification processing", Mc.Graw-Hill, Inc. (1974).
- [35] R. F. Sekerka in *Crystal: an Introduction*, ed. p. Hartman, North-Holland Publ. Co. (1973), p. 411.

*Corresponding author: sanca@infim.ro